



ELSEVIER

Available online at [www.sciencedirect.com](http://www.sciencedirect.com)

SCIENCE @ DIRECT®

C. R. Mecanique 332 (2004) 613–618



# The mixing layer instability of wind over a flexible crop canopy

Charlotte Py<sup>a</sup>, Emmanuel de Langre<sup>a</sup>, Bruno Moulia<sup>b</sup>

<sup>a</sup> *Département de mécanique, LadHyX, CNRS-École polytechnique, 91128 Palaiseau cedex, France*

<sup>b</sup> *Unité d'Ecophysiologie des Plantes Fourragères, INRA, 86600 Lusignan, France*

Received 29 September 2003; accepted 9 March 2004

Available online 14 May 2004

Presented by Évariste Sanchez-Palencia

---

## Abstract

A coupled fluid-structure model is proposed to study the dynamics of a flexible crop canopy exposed to wind. The canopy is represented by an elastic continuous medium and coupled to the wind mixing layer through a drag load. The mixing layer instability is shown to remain the principle instability mechanism but its characteristics are modified when taking into account the flexible canopy. The size of the coherent structures is decreased as well as the instability growth rate. **To cite this article:** *C. Py et al., C. R. Mecanique 332 (2004).*

© 2004 Académie des sciences. Published by Elsevier SAS. All rights reserved.

## Résumé

**Instabilité de couche de mélange dans le vent sur un couvert végétal souple.** Un modèle couplé fluide-structure est proposé pour l'étude de la dynamique d'un couvert végétal souple soumis au vent. Le couvert est représenté par un milieu élastique et couplé à la couche de mélange du vent par une force de traînée. L'instabilité de couche de mélange reste le mécanisme principal d'instabilité, mais ses caractéristiques sont modifiées par la prise en compte du couvert souple : la taille des structures cohérentes est réduite ainsi que le taux d'amplification de l'instabilité. **Pour citer cet article :** *C. Py et al., C. R. Mecanique 332 (2004).*

© 2004 Académie des sciences. Published by Elsevier SAS. All rights reserved.

*Keywords:* Fluid mechanics; Fluid structure interactions; Plant biomechanics; Mixing layer instability

*Mots-clés :* Mécanique des fluides ; Interactions fluide structure ; Biomécanique des plantes ; Instabilité de couche de mélange

---

## Version française abrégée

On sait que les couverts végétaux soumis au vent sont le siège d'une instabilité de type couche de mélange menant à la création de larges structures cohérentes qui se propagent [1,2]. Nous proposons ici un modèle couplé pour l'étude de la dynamique des couverts végétaux souples soumis au vent. Le couvert végétal est traité comme

---

*E-mail addresses:* [cpy@ladhyx.polytechnique.fr](mailto:cpy@ladhyx.polytechnique.fr) (C. Py), [delangre@ladhyx.polytechnique.fr](mailto:delangre@ladhyx.polytechnique.fr) (E. de Langre), [moulia@lusignan.inra.fr](mailto:moulia@lusignan.inra.fr) (B. Moulia).

un milieu élastique équivalent, et sa dynamique est régie par une équation d'onde (1) prenant en compte les effets d'inertie, de raideur en flexion et de contacts entre plantes [4]. Le mouvement du couvert est induit par une force de traînée agissant sur chaque plante. Le flux de vent est décrit par les équations d'Euler ((2) à (5)) dans lesquelles un terme source correspondant à la traînée est ajouté. On étudie la stabilité d'un écoulement de base représenté par un profil en lignes brisées  $U_b$  (Fig. 1), caractéristique des configurations de couche de mélange. On aboutit à la relation de dispersion (6) gouvernant l'ensemble du problème couplé.

On procède à une analyse de stabilité temporelle. En prenant un coefficient de traînée nul, la branche temporelle la plus amplifiée se confond avec la branche de Kelvin–Helmholtz (Fig. 2). L'introduction de la traînée a pour conséquence, par effet dissipatif, la diminution du taux d'amplification de l'instabilité. On étudie l'influence des caractéristiques mécaniques du couvert végétal sur les propriétés de l'instabilité. La forme de la branche temporelle est significativement modifiée en fonction de la souplesse en flexion du couvert (Fig. 3). La longueur d'onde la plus amplifiée diminue en fonction de la souplesse en flexion du milieu (Fig. 4). Pour un champ de luzerne soumis au vent, la longueur d'onde est 25 % plus petite qu'elle ne serait pour un couvert rigide équivalent. Enfin, la longueur d'onde diminue également en fonction de la souplesse de contact entre plantes, mais de manière moins significative (Fig. 5).

## 1. Introduction

Lodging of crops and thigmomorphogenesis, which is the effect of wind on plants growth, have brought a large interest on the study of wind-induced plant motions [1–3]. Wind flow over a vegetal canopy is turbulent and leads to oscillatory plant motions. The mean wind velocity profile is known to be inflected at the top of the canopy, as a result of the momentum absorption by drag on the leaves [2]. The induced shear is at the origin of an instability mechanism similar to that of a mixing layer. This yields the formation of large scale coherent flow structures propagating over the canopy [1,2]. Previous studies of wind-induced plant motions have represented the canopy as a set of mechanical oscillators [3], with elastic interactions [4], and have considered simple wind load models.

In this Note, we propose a fully coupled fluid-structure model to study the dynamics of a flexible canopy exposed to wind. A mixing layer configuration with a broken line flow profile represents the wind flow over and inside the canopy. The flexible canopy is modeled by a wave equation following Doaré et al. [4]. The fluid-structure coupling is realized through a drag load. We identify the main instability mechanism of the coupled problem, and study the effect of the mechanical characteristics of the canopy on the instability properties in the particular case of an alfalfa field.

## 2. The model

The vegetal canopy is composed of an infinite row of identical plants with elastic contacts, Fig. 1. Following Doaré et al. [4], it is modeled as an equivalent continuous medium, with mass  $m$ , flexion stiffness  $r$  and contact stiffness  $a$ . The position of any point of the canopy is described by the horizontal displacement  $\underline{X}(x, y, t) = \chi(y)Q(x, t)\underline{e}_x$ ,  $\chi$  being a mode shape, and  $Q$  the corresponding generalized displacement. The canopy movement results from a local drag force, acting on the equivalent surface of each plant and dependent on the difference between the local wind velocity and the horizontal plant velocity. This drag force is then projected on the modal shape  $\chi$ . The dynamics of the canopy is thus governed by the following wave equation:

$$m \frac{\partial^2 Q}{\partial t^2} + r Q - a \frac{\partial^2 Q}{\partial x^2} = \int_0^h \frac{1}{2} \rho C D [(\underline{U} - \dot{\underline{X}}) \cdot \underline{e}_x]^2 \chi \, dy \quad (1)$$

where  $C$  is a drag coefficient and  $D$  an effective diameter of a plant.

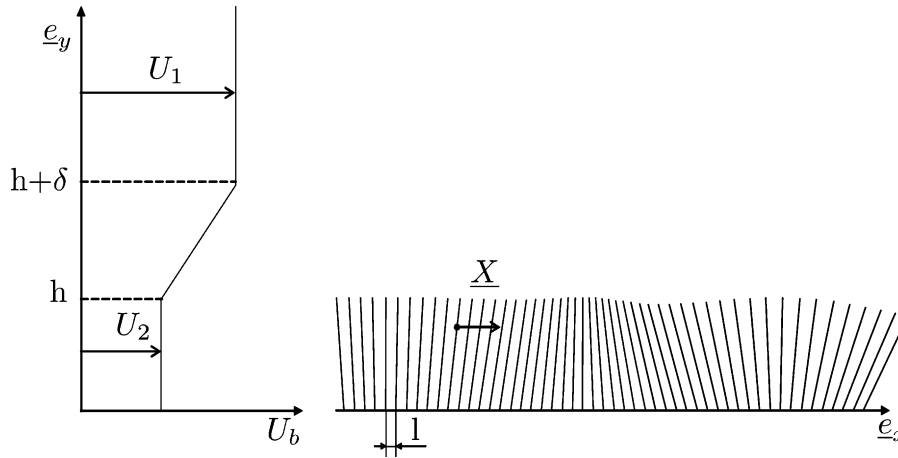


Fig. 1. Basic flow  $U_b$  and model of the crop canopy.

Fig. 1. Profil de référence  $U_b$  et modèle du couvert végétal.

The wind velocity  $\underline{U}$  is governed by the Euler equations within and above the canopy. A source term corresponding to the drag effect is added to the momentum equation. We neglect here the effect of fluid viscosity since the mixing layer instability mechanism is known to be inviscid [5].

In order to investigate the stability of a given basic state, we consider the small perturbations  $u, v, p, q$  associated respectively with a basic velocity profile  $U_b$ , pressure  $P_b$ , and canopy displacement  $Q_b$ . We use here a broken line profile  $U_b(y)$  defined by a vorticity thickness  $\delta$  and a shear parameter  $R = (U_1 - U_2)/2U$  with the mean velocity  $U = (U_1 + U_2)/2$  (see Fig. 1). This profile is commonly used to model mixing layer configurations and has been shown to capture the main characteristics of the instability [5]. The momentum and mass balance for the flow and the wave equation for the canopy may be developed at the first order in terms of the perturbations which yields the set of coupled equations:

$$\frac{\partial u}{\partial t} + U_b \frac{\partial u}{\partial x} + \frac{\partial U_b}{\partial y} u = -\frac{1}{\rho} \frac{\partial p}{\partial x} - CU_2 \frac{D}{l^2} \left( u - \chi \frac{\partial q}{\partial t} \right) \tag{2}$$

$$\frac{\partial v}{\partial t} + U_b \frac{\partial v}{\partial x} = -\frac{1}{\rho} \frac{\partial p}{\partial y} \tag{3}$$

$$\nabla \cdot \underline{u} = 0 \tag{4}$$

$$m \frac{\partial^2 q}{\partial t^2} + rq - a \frac{\partial^2 q}{\partial x^2} = \int_0^h \rho CU_2 D \left( u - \chi \frac{\partial q}{\partial t} \right) \chi dy \tag{5}$$

The drag coefficient  $C$  in (2) is set to zero outside the canopy ( $y > h$ ). We use here a linear mode shape  $\chi(y) = y/h$ . A traveling wave solution is sought in the form:  $(u, v, p, q) = (\hat{u}, \hat{v}, \hat{p}, \hat{q}) e^{i(kx - \omega t)}$ . Assuming the flow to be irrotational, the corresponding dispersion relation is obtained:

$$D(k, \omega) = -m\omega^2 + r + ak^2 - \frac{1}{3}(\rho C D U_2) i \omega h + D_{\text{fluid}} = 0 \tag{6}$$

with

$$D_{\text{fluid}} = \rho(CDU_2)^2(s - c/kh) / [ckl^2(U_2k - \omega) - ickCDU_2 + skl^2(\Delta - A(U_2k - \omega))]$$

$$A = (1 + Y)/(1 - Y), \quad Y = e^{2k\delta}(1 - 2(U_1k - \omega)/\Delta)$$

$$c = \cosh(kh), \quad s = \sinh(kh), \quad \Delta = (U_2 - U_1)/\delta$$

### 3. Analysis and results

We analyze the temporal stability of propagating waves by calculating numerically the growth rate  $\omega_i = \text{Im}(\omega)$  associated with a given real wavenumber  $k$  [5] through the dispersion relation (6). Only the most unstable branch  $\omega_i = f(k)$  is considered. The temporal analysis is performed using experimental values for the parameters of the model. These are taken from experiments on alfalfa [4] and wind characteristics over a crop canopy [1]. We use here:  $m/(\rho\delta^3) = 0.007$ ,  $r/(\rho\delta U^2) = 0.009$ ,  $a/(\rho\delta^3 U^2) = 1.5 \times 10^{-5}$ ,  $h/\delta = 1$ ,  $l/\delta = 0.1$ ,  $D/\delta = 0.02$ ,  $C = 1$ ,  $R = 0.5$ . Fig. 2 shows the temporal branch derived from the dispersion relation.

The growth rate may be compared with that arising from uncoupled fluid and solid dynamics by setting the drag coefficient  $C$  to zero. In that case, the unstable branch is that of the Kelvin–Helmholtz instability in a bounded domain, Fig. 2. Then, by setting  $h/\delta$  equal to infinity, the Kelvin–Helmholtz temporal branch for a broken-line profile in an infinite medium is recovered, with the most amplified wavenumber at  $k\delta = 0.8$  [5]. We may therefore assert that taking into consideration the flexible canopy through the drag term modifies the shape of the Kelvin–Helmholtz temporal branch, but this latter is still the most amplified. The mixing layer instability therefore remains the main mechanism of vortex formation over canopies, even when considering the drag on the flexible plants. The first effect of the coupling by a drag force is to decrease the maximum growth rate of the instability: dissipative effects in mixing layers are indeed known to be stabilizing, see for instance [6].

The effect of the mechanical characteristics of the plants on the instability mechanism is now investigated by comparing the most amplified temporal branch between a flexible canopy and a rigid one. Fig. 3 shows that the

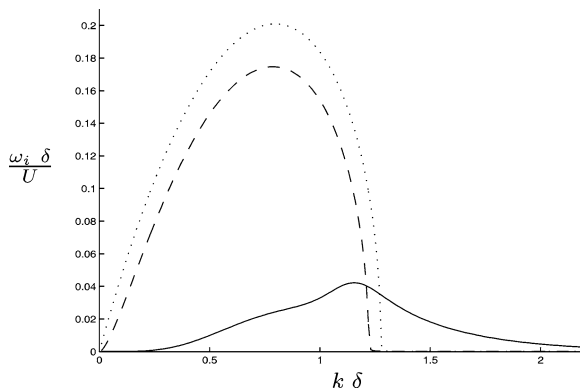


Fig. 2. Dimensionless temporal branch. (—) model with experimental values of the parameters, (– –)  $C = 0$ : Kelvin–Helmholtz branch in a bounded medium, (···) Kelvin–Helmholtz branch in an infinite medium.

Fig. 2. Branche temporelle adimensionnelle. (—) modèle avec valeurs expérimentales des paramètres, (– –)  $C = 0$ : branche Kelvin–Helmholtz dans un milieu borné, (···) branche Kelvin–Helmholtz dans un milieu infini.

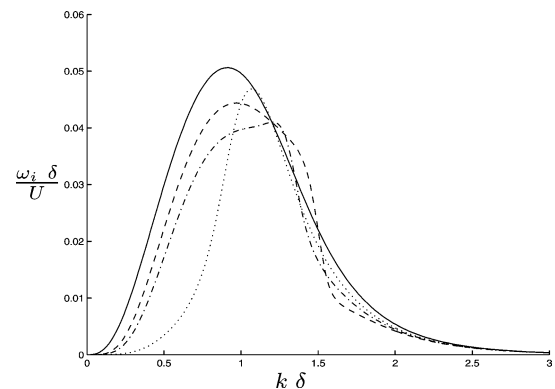


Fig. 3. Temporal branch for different values of the dimensionless flexural compliance  $s^* = \rho U^2 \delta / r$ : (—)  $s^* = 0$ , (– –)  $s^* = 45$ , (– · –)  $s^* = 66$ , (···)  $s^* = 350$ .

Fig. 3. Branche temporelle pour diverses valeurs de la souplesse en flexion adimensionnelle  $s^* = \rho U^2 \delta / r$ : (—)  $s^* = 0$ , (– –)  $s^* = 45$ , (– · –)  $s^* = 66$ , (···)  $s^* = 350$ .

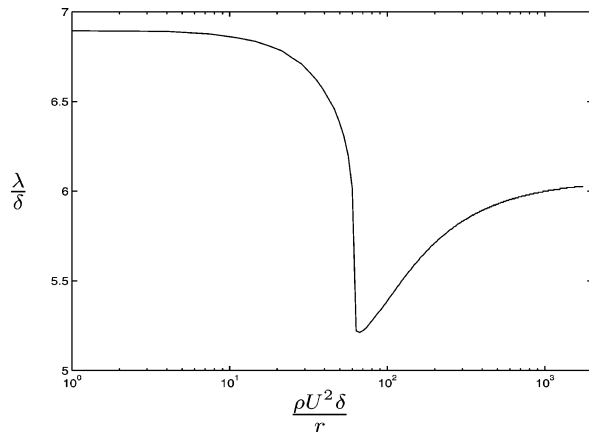


Fig. 4. Most amplified wavelength as a function of the dimensionless flexural compliance of the plants.

Fig. 4. Longueur d'onde la plus amplifiée en fonction de la souplesse en flexion adimensionnelle des plantes.

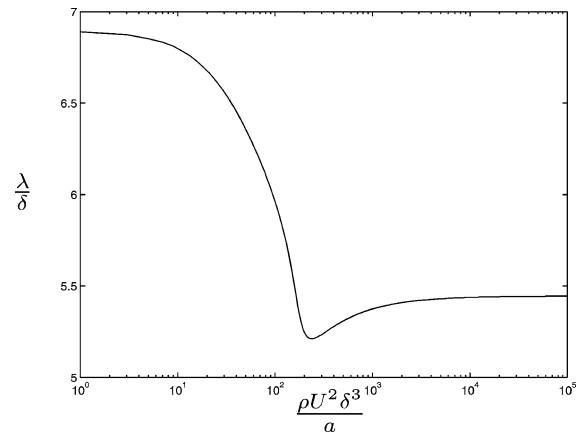


Fig. 5. Most amplified wavelength as a function of the dimensionless contact compliance.

Fig. 5. Longueur d'onde la plus amplifiée en fonction de la souplesse de contact adimensionnelle.

shape of the temporal branch is significantly modified when the flexural compliance of the plants is varied. This results in an evolution of the most amplified wavenumber, shown (Fig. 4) in terms of the corresponding wavelength  $\lambda$ , as a function of the dimensionless flexural compliance  $s^* = \rho U^2 \delta / r$ . The crop compliance has a nonregular but significant effect on the size of the coherent structures arising from the instability. For the particular case of an alfalfa canopy using a 3 m/s wind ( $s^* \simeq 100$ ), the wavelength is approximately 25% smaller than it would be for an equivalent rigid canopy.

The compliance of the contacts between plants also influences the most amplified wavelength (see Fig. 5). The effect is nonregular and globally decreasing, as for the flexural compliance. For an alfalfa canopy exposed to 3 m/s wind ( $\rho U^2 \delta^3 / a \simeq 5 \times 10^4$ ), the wavelength is about 13% smaller than it would be for an equivalent flexible canopy with rigid contacts. Note that in this range of parameters the dependence with contact compliance is small. In fact in the dispersion relation, see (6),  $ak^2$  is then much smaller than  $r$ , the flexural stiffness term. In denser canopies, such as in wheat, the contact compliance is expected to play a more significant role.

When the flexural compliance or the interaction compliance tend to zero, a common limit wavelength is obtained, see Figs. 4 and 5, at  $\lambda \simeq 6.9$ . This corresponds to a Kelvin–Helmholtz instability with a drag force but no motion of the canopy. In the dispersion relation, Eqn. (6), the existence of very large terms originating from the crop stiffness,  $r$  and  $ak^2$ , requires that the corresponding solution in terms of  $(\hat{u}, \hat{v}, \hat{p}, \hat{q})$  is then dominated by fluid motion ( $\hat{q} \simeq 0$ ).

#### 4. Conclusion

The mixing layer instability is known to be responsible for the existence of strong coherent motions of canopies exposed to wind [2]. We have solved here the interaction problem where the mixing layer dynamics is fully coupled with the motion of the canopy. The main conclusion is that for realistic values of the crop flexibility the mixing layer instability persists but its characteristics are significantly modified. The most amplified wavelength is reduced, as well as the corresponding growth rate of the instability. This may explain some discrepancies between the original mixing layer model and measurements of the size of coherent structures observed in wind over various canopies such as corn or forest as reported in [1].

**References**

- [1] J.J. Finnigan, Turbulence in plant canopies, *Annu. Rev. Fluid Mech.* 32 (2000) 519–571.
- [2] M.R. Raupach, J.J. Finnigan, Y. Brunet, Coherent eddies and turbulence in vegetation canopies: the mixing layer analogy, *Boundary-Layer Meteorology* 78 (1996) 351–382.
- [3] T. Farquhar, J. Zhou, H. Haslach, A possible mechanism for sensing crop canopy ventilation, in: F. Barth, J. Humfrey, T. Secomb (Eds.), *Sensors and Sensing in Biology and Engineering*, Springer, Wien, 2003, Chapter 15.
- [4] O. Doaré, B. Moulià, E. de Langre, Effect of plant interaction on wind-induced crop motion, *Trans. ASME J. Biomech. Engrg.* (2004) in press.
- [5] P. Huerre, M. Rossi, Hydrodynamic instabilities in open flows, in: C. Godrèche, P. Manneville (Eds.), *Hydrodynamics and Nonlinear Instabilities*, Cambridge University Press, Cambridge, 1998, pp. 81–294.
- [6] R.L. Panton, Introduction to stability and transition, in: *Incompressible Flow*, second ed., Wiley-Interscience, New York, 1996, Chapter 22.